Catal Lett (2017) 147:215–220
DOI 10.1007/s10562-016-1907-2

Ternary Transitional Metal Chalcogenide Nanosheet with Significantly Enhanced Electrocatalytic Hydrogen-Evolution Activity

Jinxia Wu[1] · Jiali He[1] · Fan Li[1] · Xin Hu[1]

Received: 10 August 2016 / Accepted: 3 November 2016 / Published online: 12 November 2016

Abstract Electrochemical production of hydrogen from water holding tremendous promise for clean energy has been directed to the search for non-noble metal based and earth-abundant catalysts. Here we report dramatically enhanced HER catalysis of ternary *I*-Cu_2WS_4 nanosheets from chemically exfoliated via lithium intercalation. Structural characterization and electrochemical study confirmed that the enhanced electrocatalytic activity of *I*-Cu_2WS_4 nanosheets is associated with the larger surface area to provide an easy path for the hopping of electrons. This study opens a new way for the development of ternary highly active non-noble electrocatalysts for hydrogen production from water splitting.

Graphical Abstract

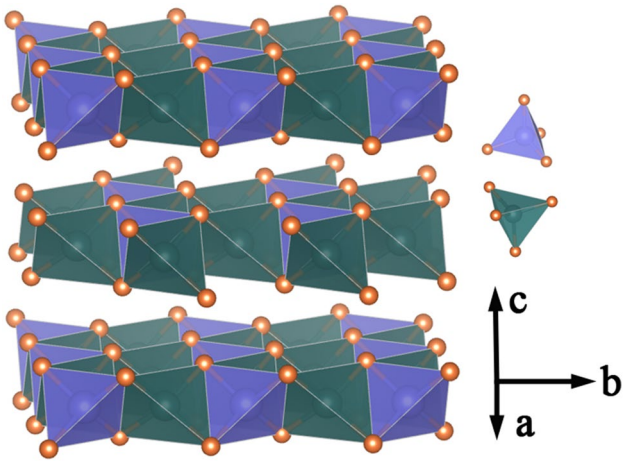

Keywords Catalysis · Hydrothermal synthesis · Nanostructure · Hydrogen evolution reaction · Ternary transitional metal chalcogenides · AFM · Thin layers

1 Introduction

Developing green energy conversion material systems will greatly alleviate the energy crisis and the impaction on our life and environment. The electrochemical catalytic decomposition of water into hydrogen is friendly environmental energy conversion strategy [1–4]. However, among the many hydrogen evolution reaction (HER) electrocatalysts, the best HER performance has been achieved using prohibitively very expensive platinum electrodes, severely impeding their widespread usage. During the past few years, extensive efforts have been done to develop non-noble HER. Although the identification of XS_2 (X = Mo,

Electronic supplementary material The online version of this article (doi:10.1007/s10562-016-1907-2) contains supplementary material, which is available to authorized users.

✉ Xin Hu
81387429@qq.com

[1] College of Chemistry and Chemical Engineering, Xinjiang Normal University, Urumqi, Xinjiang 830054, People's Republic of China

W) compounds as potential efficient catalysts for HER has opened up an exciting new path for the field,[5–10] the scientific community has been still actively understanding of the HER mechanism at the molecular level that guide the design of better catalysts and make the hydrogen production more economic and competitive.

Ternary transitional metal chalcogenides which possess a variety of intriguing chemical and physical properties [11–14] are common complexes that have seldom been explored for electrocatalysis despite past suggestion that they could be efficient HER catalysts. The exploration of their novel and useful HER properties has great scientific and practical meanings [15]. Lately, it was reported that introducing certain transition metal ions result in encouraging HER activity for the significant improvement both in the intrinsic catalytic properties and effective electrochemical surface area of Mo/W sulfides or nitrides when they are incorporated into the host lattice [16]. For example, the ternary $Co_{0.6}Mo_{1.4}N_2$ [17] is expected that the layered nature of this structure allows the 3d transition metal to tune the electronic states of molybdenum at the catalyst surface without disrupting the catalytic activity and that alternative substitutions on the octahedral site of this structure type may lead to even better HER activity, in which abundant H species can be identified on the surface which bond strongly with molybdenum atoms. However, guided by the "volcano plot", [18] it is revealed that strong Mo–H bond could impede hydrogen release from the active sites and fail to evolve hydrogen [19–21]. Similarly, the bimetallic Ni–Mo–N_x catalyst may be more amenable to optimization, though catalytically active samples were found to contain a mixture of an ionic rock salt phase (γ–Mo_2N-type) and a Ni_2Mo_3N (Mo_3Al_2C-type) phase, and it has not yet been established which phase is responsible for the observed HER activity [19]. In particular, it has been recently reported that the layered ternary sulfide copper-molybdenum-sulfide (Cu_2MoS_4) shown good HER catalytic performance, but the active site responsible for the HER is presently not completely elucidated [22]. This is partly because the structure is too complex to easily identify hydrogen adsorption sites. Therefore, much simpler crystal systems and/or more controlled surface conditions can help precisely identify the role of the catalyst in elctrocatalytic water splitting.

Both experimental and theoretical works suggest that the catalytic activity of ternary transitional metal chalcogenides may be more amenable to optimization by the 3d transition metals tune the electronic states of Mo/W [19, 20]. Ternary transitional metal chalcogenides could be a new class of efficient electrocatalysts and worthy of further in-depth study because they not only provide new opportunities for exploring advanced catalytic functional composites but also expand and enrich the family of high performance HER catalysts. Although a lot of ternary transitional metal chalcogenides were synthetised, there have only been a few scattered studies focusing on them based HER electrocatalysts to date [22]. Furthermore, their electrocatalytic mechanism such as identifying the active site is also far from satisfactory with the scientific research needs. For the HER, a key point lies in the identification of potential active sites. Identifying the active site will certainly come with a deeper fundamental understanding of the reaction and its mechanism and is critical to designing and developing improved catalytic materials because through proper compositional and structural engineering, the catalyst is able to catalyze hydrogen generation at small onset overpotentials with remarkable durability [23, 24]. However, progress in the field of ternary (or heterogeneous) catalysis is usually hampered by the difficulty of identifying the active site on a catalyst surface and prevented the massive deployment of these materials for hydrogen production.

The two-dimensional (2D) nanosheets have recently sparked worldwide interests owing to their unique electronic structures and physical properties compared with the corresponding bulk samples [25, 26]. With their high surface area-to-volume ratio, nanosheets provide an ideal electrocatalyst structure for determining the reaction mechanisms. Herein, we investigate the body-centred copper-tungsten-sulfide (*I*-Cu_2WS_4) 2D nanosheet as a model for mechanistic studies of ternary transitional metal chalcogenides for the HER, which has a square planar arrangement formed by interlinked copper and tungsten atoms tetrahedrally coordinated to bridging sulfur atoms. The tungsten atoms in one layer lie above metal vacancies in adjacent layers, minimising electrostatic interactions between them [27, 28]. The surface of every sheet is thoroughly comprised by the S atoms, which sandwiched Cu/W atoms in the center of individual monolayers. The highly crystalline ternary transitional metal sulfide with the unique atom alignment manner were put forward as an excellent platform to promote the hydrogen evolution activity through affording abundant catalytically active sites and increased 2D conductivity. The possible catalytic mechanism involved in the HER is also explained.

2 Results and Discussion

In this work, the *I*-Cu_2WS_4 nanosheets were fabricated by chemical exfoliation of the bulk material through ultrasonicating the Li-intercalated *I*-Cu_2WS_4 precursor in water, giving the ternary *I*-Cu_2WS_4 freestanding nanosheets. The X-ray powder pattern (Fig. 1a) showed that the product of the reaction was a form of *I*-Cu_2WS_4, identical to that previously reported,[29] containing layers of edge-sharing WS_4 and CuS_4 tetrahedrals separated by a van der Waals

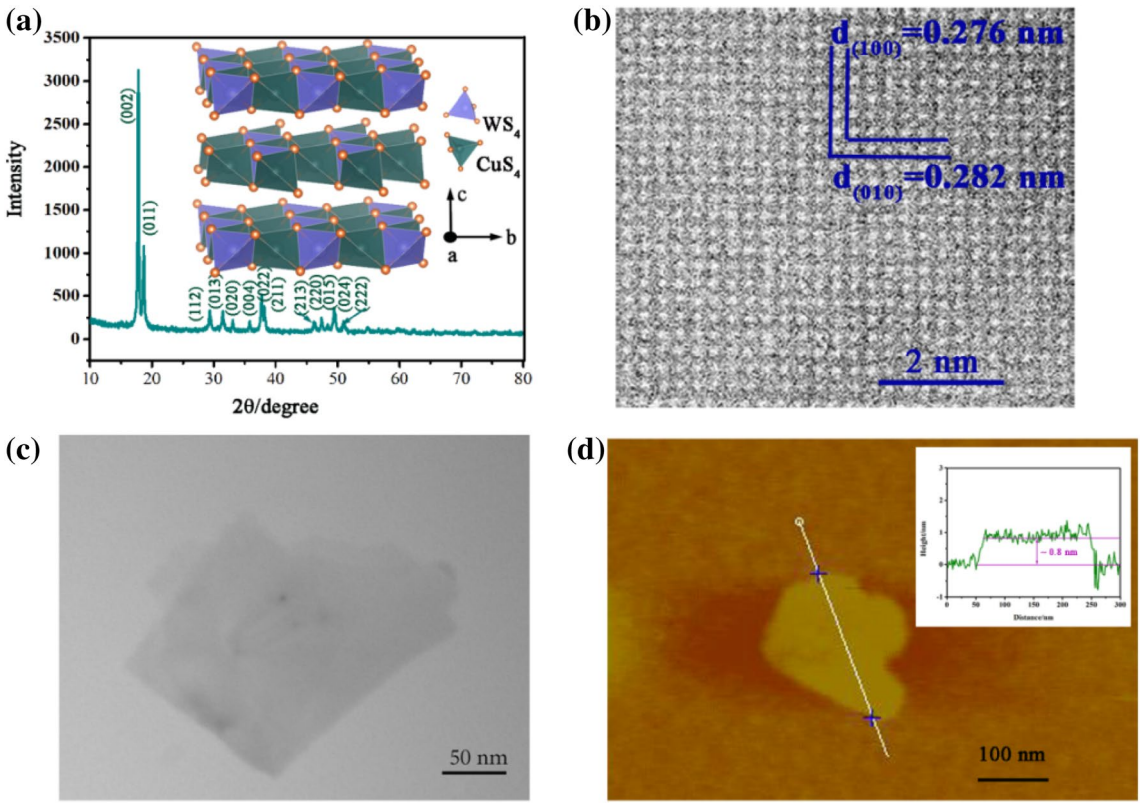

Fig. 1 **a** XRD pattern of the product. *Inset* the structure of *I*-Cu_2WS_4. **b** HRTEM image of the *I*-Cu_2WS_4 nanosheets. **c** TEM image of an individual nanosheet. **d** AFM image revealing the atomic thickness of the *I*-Cu_2WS_4 nanosheets. *Inset* the corresponding height image of the nanosheet in (**d**)

gap (Fig. 1a). Meanwhile, as depicted in Supporting Figure S1, the X-ray photoelectron spectroscopy (XPS) reveals that the product consisted of the elements W, Cu and S. Two characteristic peaks arising from Cu 2p1/2 and Cu 2p3/2 orbitals are located at 952.30 and 932.80 eV, suggesting the dominance of Cu(I) in the product [30]. The peaks at 35.33 and 33.16 eV correspond to W 4f5/2 and W 4f7/2 [31]. While the S 2p region exhibits primarily a single doublet with the 2p3/2 peak at 162.52 eV, which is consistent with −2 oxidation state of sulfur [32]. The HRTEM image (Fig. 1b) was performed on a typical ultrathin nanosheet, showing the high degree of [001] orientation. In addition, Figure S2 displays the scanning electron microscopy (SEM) image of bulk *I*-Cu_2WS_4, showing a regular morphology with lateral size of about 2 μm and a thickness of about 0.5 μm. In contrast, the transmission electron microscopy (TEM) image of the as-exfoliated products clearly shows a 2D sheet-like structure with a size about 200 nm (Fig. 1c), significantly differing from the morphology of larger and more regular bulk *I*-Cu_2WS_4, which is further verified by the atomic force microscopic (AFM) image and the corresponding height profile shown in Fig. 1d. The AFM image and the corresponding height profile display the sheet-like morphology with a height of about 0.8 nm, which agrees well with the 0.76 nm of a double-layered *I*-Cu_2WS_4 slab along the [001] direction. Thus, taking into account the evidence from each characterization technique, we can summarize that the *I*-Cu_2WS_4 nanosheets possess uniform two-dimensional morphology, atomically thickness and large surface areas.

In order to verify the structural benefits of the nanosheet and survey the HER mechanism for *I*-Cu_2WS_4 catalysts, the HER measurements with chemically exfoliated *I*-Cu_2WS_4 nanosheets thin film as the catalyst on glassy carbon electrode(GCE) with 0.285 mg cm^{-2} was carried out using the standard three-electrode electrochemical configuration in 0.5 M H_2SO_4 electrolyte deaerated with H_2. For comparison, the current density versus voltage (j versus V) for the nanosheets and bulk *I*-Cu_2WS_4 powder samples along with glassy carbon as a reference were all measured. The Pt reference trace was recorded using a Pt wire as the working electrode [33]. As shown in Fig. 2a, benefiting from the 2D structure, the HER activity was dramatically enhanced in the as-exfoliated nanosheets as compared to their bulk material. The *I*-Cu_2WS_4 nanosheets exhibit substantially improved

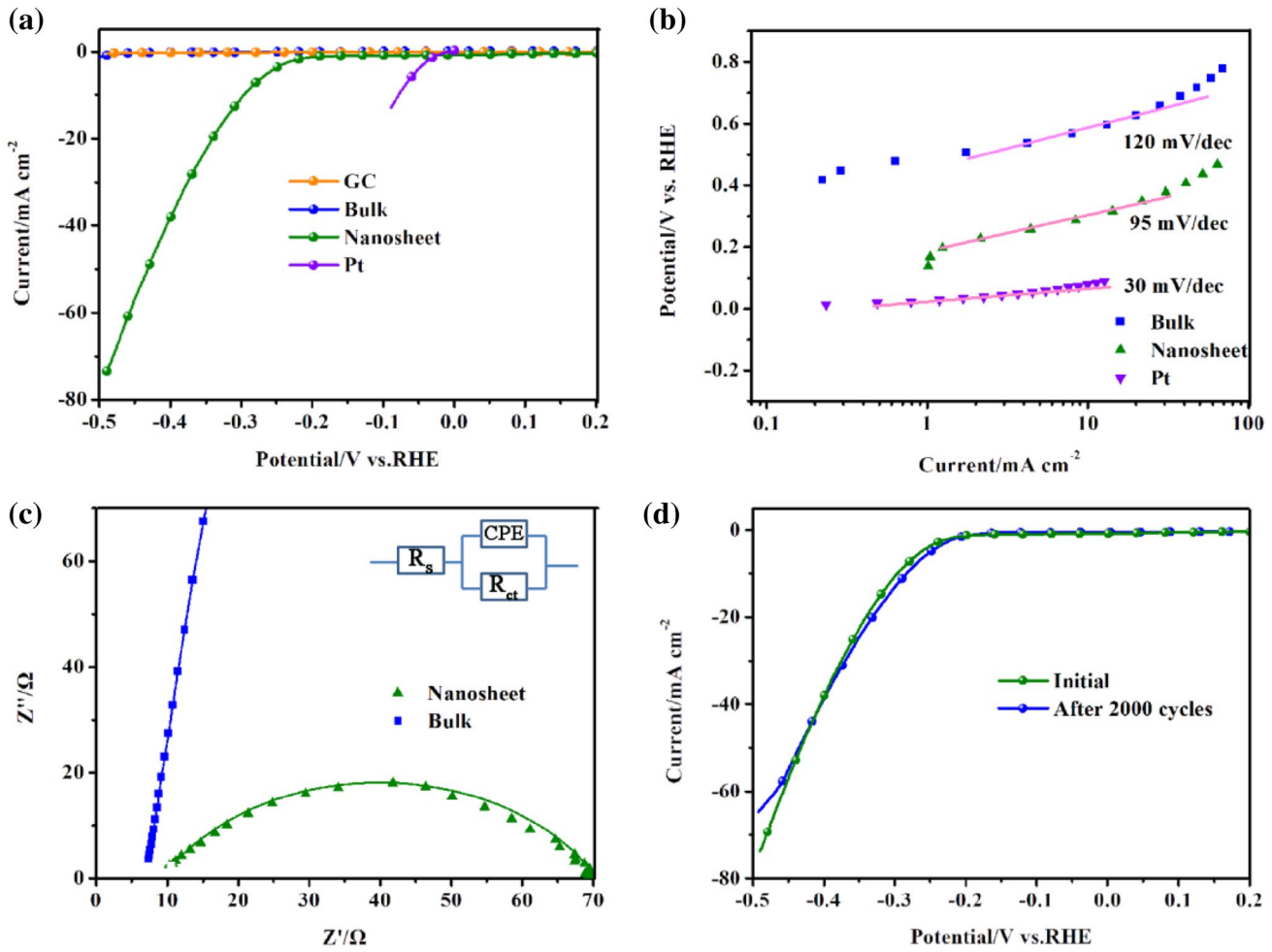

Fig. 2 **a** Polarization curves obtained from glassy carbon electrodes modified with different *I*-Cu_2WS_4 catalysts. **b** The corresponding Tafel plots recorded with a catalyst loading of 0.285 mg cm^{-2}; scan rate is 50 mV s^{-1}. **c** Nyquist plots of different samples. The fitted curves are presented by *solid lines*. **d** Polarization curves revealing that negligible degradation of HER activity is observed for *I*-Cu_2WS_4 nanosheets even after 2000 CV cycles

electrocatalytic activity with low onset overpotentials of ~170 mV (Fig. 2a), beyond which the cathodic current rises rapidly under more negative potentials. In contrast, the bulk material exhibits serious fade of HER activity with high onset overpotential value of ~500 mV in the same condition. Interestingly, the *I*-Cu_2WS_4 nanosheets electrodes show HER characteristics that are consistent with reported WS_2 and MoS_2 with typical overpotential of 150–200 mV whereas the bulk powder exhibits poor catalytic activity [9]. Cathodic current density is considered as an important evaluating criterion for HER activity. The as-exfoliated nanosheet exhibits an extremely large cathodic current density of 74 mA cm^{-2} at $\eta = 500$ mV, showing 74-fold enhancement compared with that of the bulk counterpart, confirming the excellent activity of the atomically-thin *I*-Cu_2WS_4 nanosheets. The bulk *I*-Cu_2WS_4 particles have smaller surface areas and exhibited very lower catalytic activities, indicating that the surface area is a crucial structural parameter dominating the HER, as reported widely in the literature. In addition, upon lithium intercalation, layers of *I*-Cu_2WS_4 become charged due to the electron transfer between *n*-BuLi and *I*-Cu_2WS_4. Some of these negative charges react with water during the exfoliation process, but a fraction remain on the nanosheets, rendering them negatively charged [10]. The removal of charged impurities from the surface of *I*-Cu_2WS_4 nanosheets facilitates electron transfer between the nanosheets and the protons in the electrolyte solution during HER. Moreover, the 2D configuration with extremely large surface area provided intimate contact with the GC electrode and high interfacial contact area with the electrolyte, thus guaranteeing fast interfacial charge transfer and facile electrochemical reactions as well as low corrosion rates. As discussed

above, the significantly improved catalytic activity of *I*-Cu_2WS_4 nanosheets from a potent combination of specific structural properties, namely large surface areas and nanosized crystallites, contributing to the high abundance of available catalytic active sites and smaller charge-transfer resistances of the electrode.

It is well known that the Tafel slope is an inherent property of the catalyst which is determined by the rate-limiting step of the HER. Further insight into the catalytic activity of the *I*-Cu_2WS_4 nanosheets electrodes was obtained by extracting the slopes from the Tafel plots shown in Fig. 2b. The Tafel slope of 95 mV decade^{-1} for the *I*-Cu_2WS_4 nanosheet is much smaller than the bulk counterpart of 120 mV decade^{-1}, which suggests that the rate determining step is adsorption of protons on the catalyst surface. Typically, the exchange current density (j_0) is expected to be proportional to catalytically active surface area. The exchange current density of *I*-Cu_2WS_4 nanosheets is calculated to be about 177 mA/cm^2, 6.8 times of that of bulks (26 mA/cm^2) (Figure S4). We attribute this high j_0 to the unique exfoliated nanosheet nanostructure that affords plenty of highly accessible reactive sites. Furthermore, electrochemical double layer capacitances (C_{dl}) are measured to evaluate the effective surface area of various catalysts at the solid–liquid interface with cyclic voltammetry (Figure S5). The nanosheet exhibits much larger (C_{dl} of 347 μF) than the bulk, indicating the high exposure of effective surface area, which is responsible for the excellent HER activity.

Catalytic stability is another significant criterion for HER catalysts. To assess the long-term durability of the catalyst, the catalytic stability of our *I*-Cu_2WS_4 nanosheet is characterized by continuous cyclic voltammetry performed between −0.5 V and 0.2 V versus RHE at 50 mV/s scan rate for 2000 cycles (Fig. 2d). At the end of the cycling procedure, the current densities show that the catalyst affords similar to the initial cycle with negligible loss of the cathodic current, indicating that the *I*-Cu_2WS_4 catalysts maintained its unique nanosheet structure over a long time in an acidic environment. Overall, these electrochemical results demonstrate that as-exfoliated *I*-Cu_2WS_4 nanosheets could be effective electrocatalysts for HER.

The enhanced electrocatalytic activity of *I*-Cu_2WS_4 nanosheets may arise from two reasons. Firstly, the ultrathin thickness and 2D planar nanostructure with huge surface area are in favor of the catalyst full contact with the electrolyte, effectively shortened the diffusion path of electrolyte ions, facilitating fast interfacial charge transfer and electrochemical reactions. Secondly, 2D nanosheet with huge surface area increased the density of active sites for the redox reaction. Therefore, the *I*-Cu_2WS_4 nanosheet catalyst shows excellent electrocatalytic performance.

3 Conclusions

In conclusion, we have demonstrated that facile chemically exfoliation can transform bulk, a poor catalyst, into *I*-Cu_2WS_4 nanosheets, an active and stable catalyst for HER for the first time. Analyses indicate that the enhanced electrocatalytic activity of the nanosheet is correlated to the the ultrathin thickness and 2D planar nanostructure. In acids, the *I*-Cu_2WS_4 nanosheets catalyst exhibited efficient and durable activity for the hydrogen evolution reaction, with a small onset overpotential of approximately 170 mV and a Tafel slope of 95 mV decade^{-1}. Our present study offers us a novel inexpensive hydrogen-evolving electrocatalyst with excellent activity and durability.

Acknowledgements The research was financially supported by Natural Science Foundation of Xinjiang (2016D01A055).

References

1. Lewis NS, Nocera DG (2006) Proc Natl Acad Sci USA 103:15729
2. Turner JA (2004) Synthesis of the NNTAs Electrode: the NNTAs electrode was obtained. Science 305:972–974
3. Zeng M, Li YG (2015) Recent advances in heterogeneous electrocatalysts for the hydrogen evolution reaction. J Mater Chem A 3:14942–14962
4. Faber MS, Jin S (2014) Earth-abundant inorganic electrocatalysts and their nanostructures for energy conversion applications. Energy Environ Sci 7:3519–3542
5. Voiry D, Yamaguchi H, Li JW, Silva R, Alves DCB, Fujita T, Chen MW, Asefa T, Shenoy V, Chhowalla GEM (2013) Enhanced catalytic activity in strained chemically exfoliated WS_2 nanosheets for hydrogen evolution. Nat Mater 12:850–855
6. Li YG, Wang HL, Xie LM, Liang YY, Hong GS, Dai HJ (2011) MoS_2 nanoparticles grown on graphene: an advanced catalyst for the hydrogen evolution reaction. J Am Chem Soc 133:7296–7299
7. Xie JF, Zhang JJ, Li S, Grote F, Zhang XD, Zhang H, Wang RX, Lei Y, Pan BC, Xie Y (2013) Controllable disorder engineering in oxygen-incorporated MoS_2 ultrathin nanosheets for efficient hydrogen evolution. J Am Chem Soc 135:17881–17888
8. Lukowski MA, Daniel AS, English CR, Meng F, Forticaux A, Hamers RJ, Jin S (2014) Highly active hydrogen evolution catalysis from metallic WS_2 nanosheets. Energy Environ Sci 7:2608–2613
9. Lukowski MA, Daniel AS, Meng F, Forticaux A, Li LS, Jin S (2013) Enhanced hydrogen evolution catalysis from chemically exfoliated metallic MoS_2 nanosheets. J Am Chem Soc 135:10274–10277
10. Voiry D, Salehi M, Silva R, Fujita T, Chen MW, Asefa T, Shenoy VB, Eda G, Chhowalla M (2013) Conducting MoS_2 nanosheets as catalysts for hydrogen evolution reaction. Nano Lett 13:6222–6227
11. Aup-Ngoen K, Thongtem T, Thongtem S (2013) Cyclic microwave-assisted synthesis of CuFeS2 nanoparticles using biomolecules as sources of sulfur and complexing agent. Mater Lett 101:9–12

12. Tan Y, Lin Z, Ren W (2012) Facile solvothermal synthesis of Cu_2SnS_3 architectures and their visible-light-driven photocatalytic properties. Mater Lett 89:240–242
13. Yin J, Jia J, Yi G (2013) Synthesis and photoelectric application of $AgInS_2$ clusters. Mater Lett 111:85–88
14. Zhang YC, Chen WW, Hu XY (2007) Controllable synthesis and optical properties of Zn-doped CdS nanorods from single-source molecular precursors. Cryst Growth Des 7:580–586
15. Jia Q, Zhang YC, Li J, Chen Y, Xu B (2014) Hydrothermal synthesis of Cu_2WS_4 as a visible-light-activated photocatalyst in the reduction of aqueous Cr(VI). Mater Lett 117:24–27
16. Merki D, Vrubel H, Rovelli L, Fierro S, Hu XL (2012) Fe, Co, and Ni ions promote the catalytic activity of amorphous molybdenum sulfide films for hydrogen evolution. Chem Sci 3:2515–2525
17. Cao BF, Veith GM, Neuefeind GC, Adzic RR, Khalifah PG (2013) Mixed close packed cobalt molybdenum nitrides as non-noble metal electrocatalysts for the hydrogen evolution reaction. J Am Chem Soc 135:19186–19192
18. Jakšić MM (2001) Int J Hydrogen Energy 26:559–578
19. Chen WF, Sasaki K, Ma C, Frenkel AI, Marinkovic N, Muckerman JT, Zhu YM, Adzic RR (2012) Hydrogen-evolution catalysts based on non-nobel metal nickel-molybdenum nitride nanosheets. Angew Chem Int Ed 51:6131–6135
20. Xie JF, Li S, Zhang XD, Zhang JJ, Wang RX, Zhang H, Pan BC, Xie Y (2014) Atomically-thin molybdenum nitride nanosheets exposing active surface sites for efficient hydrogen evolution. Chem Sci 5:4615–4620
21. Xiao P, Sk MA, Thia L, Ge XM, Lim RJ, Wang JY, Lima KH, Wang X (2014) Molybdenum phosphide as an efficient electrocatalyst for the hydrogen evolution reaction. Energy Environ Sci 7:2624–2629
22. Tran PD, Nguyen M, Pramana SS, Bhattacharjee A, Chiam SY, Fize J, Field MJ, Artero V, Wong LH, Loo J, Barber J (2012) Copper molybdenum sulfide: a new efficient electrocatalyst for hydrogen production from water. Energy Environ Sci 5:8912–8916
23. Cabán-Acevedo M, Stone ML, Schmidt JR, Thomas JG, Ding Q, Chang HC, Tsai ML, He JH, Jin S (2015) Efficient hydrogen evolution catalysis using ternary pyrite-type cobalt phosphosulphide. Nat Mater 14:1245–1253
24. Jaramillo TF, Jørgensen KP, Bonde J, Nielsen JH, Chorkendorff SH (2007) Ib,Identification of active edge sites for electrochemical H_2 evolution from MoS_2 nanocatalysts. Science 317:100–102
25. Zhang XD, Xie X, Wang H, Zhang JJ, Pan BC, Xie Y (2013) Enhanced photoresponsive ultrathin graphitic-phase C_3N_4 nanosheets for bioimaging. J Am Chem Soc 135:18–21
26. Zhang XD, Zhang JJ, Zhao JY, Pan BC, Kong MG, Chen J, Xie Y (2012) Half-metallic ferromagnetism in synthetic Co_9Se_8 nanosheets with atomic thickness. J Am Chem Soc 134:11908–11911
27. Liang L, Zhang JJ, Zhou YY, Xie JF, Zhang XD, Guan ML, Pan BC, Xie Y (2013) High-performance flexible electrochromic device based on facile semiconductor-to-metal transition realized by WO_3 center dot $2H_2O$ ultrathin nanosheets. Sci Rep 3:1936–1943
28. Crossland CJ, Evans JSO (2003) Synthesis and characterisation of a new high pressure polymorph of Cu_2WS_4. Chem Commun pp 2292–2293
29. Crossland CJ, Hickey PJ, Evans JSO (2005) The synthesis and characterisation of Cu_2MX4 (M = W or Mo; X = S, Se or S/Se) materials prepared by a solvothermal method. J Mater Chem 15:3452–3458
30. Tayeb KB, Lamonier C, Lancelot C, Fournier M (2012) Active phase genesis of NiW hydrocracking catalysts based on nickel salt heteropolytungstate: comparison with reference catalyst. Appl Catal B 126:55–63
31. Vlies AJVD, Kishan G, Niemantsverdriet JW (2002) Basic reaction steps in the sulfidation of crystalline tungsten oxides. J Phys Chem B 106:3449–3457
32. Zhang YC, Tang JY, Wang GL, Zhang M (2006) Facile synthesis of submicron Cu_2O and CuO crystallites from a solid metallorganic molecular precursor. J Cryst Growth 294:278–282
33. Faber MS, Dziedzic R, Lukowski MA, Kaiser NS, Ding Q, Jin S (2014) High-performance electrocatalysis using metallic cobalt pyrite (CoS_2) micro- and nanostructures. J Am Chem Soc 136:10053–10061